Ferromagnetic Interaction in an Asymmetric End-to-End Azido Double-Bridged Copper(II) Dinuclear Complex: A Combined Structure, Magnetic, Polarized Neutron Diffraction and Theoretical Study

Christophe Aronica,[a] Erwann Jeanneau,[a] Hani El Moll,[a] Dominique Luneau,*[a] Béatrice Gillon,*[b] Antoine Goujon,[b] Alain Cousson,[b] Maria Angels Carvajal,[c] and Vincent Robert*[c]

Abstract: A new end-to-end azido double-bridged copper(II) complex [Cu$_2$L$_2$(N$_3$)$_2$] (**1**) was synthesized and characterized (L=1,1,1-trifluoro-7-(dimethylamino)-4-methyl-5-aza-3-hepten-2-onato). Despite the rather long Cu–Cu distance (5.105(1) Å), the magnetic interaction is ferromagnetic with $J = +16$ cm^{-1} ($H = -JS_1S_2$), a value that has been confirmed by DFT and high-level correlated ab initio calculations. The spin distribution was studied by using the results from polarized neutron diffraction. This is the first such study on an end-to-end system. The experimental spin density was found to be localized mainly on the copper(II) ions, with a small degree of delocalization on the ligand (L) and terminal azido nitrogens. There was zero delocalization on the central nitrogen, in agreement with DFT calculations. Such a picture corresponds to an important contribution of the d$_{x^2-y^2}$ orbital and a small population of the d$_{z^2}$ orbital, in agreement with our calculations. Based on a correlated wavefunction analysis, the ferromagnetic behavior results from a dominant double spin polarization contribution and vanishingly small ionic forms.

Keywords: ab initio calculations · azides · copper · density functional calculations · magnetic properties · neutron diffraction

[a] Dr. C. Aronica, Dr. E. Jeanneau, H. El Moll, Prof. Dr. D. Luneau
Université Claude Bernard Lyon-1
Laboratoire des Multimatériaux et Interfaces (UMR 5615)
Campus de La Doua, 69622 Villeurbanne Cedex (France)
Fax: (+33)472-431-160
E-mail: luneau@univ-lyon1.fr

[b] Dr. B. Gillon, Dr. A. Goujon, Dr. A. Cousson
Laboratoire Léon Brillouin, CEA-CNRS, UMR0012, Centre d'Etudes Nucléaires
Saclay, 91191 Gif sur Yvette (France)
E-mail: gillon@cea.fr

[c] Dr. M. A. Carvajal, Dr. V. Robert
Ecole Normale Supérieure de Lyon, Laboratoire de Chimie (UMR 5182)
46, allée d'Italie, 69364 Lyon Cedex 07 (France)
E-mail: vincent.robert@ens-lyon.fr

Supporting information for this article is available on the WWW under http://www.chemeurj.org/ or from the author. The experimental spin populations of the copper 3d orbitals are given in Table S1. The corresponding spin density maps are represented in the *xy*, *yz*, and *xz* planes relative to the local axes of one copper atom in Figure S1–S3. The molecular structure of compound **2** is represented in Figure S4.

Introduction

It may seem surprising that, after decades of studies and discussions about the magnetostructural relationships of azido double-bridge copper(II) dinuclear complexes, such a simple system still requires attention. This is illustrative of how new experimental discoveries may improve our understanding of the magnetic exchange coupling mechanism. The aim of this report is to present new results that should contribute to this general effort.

Numerous azido-bridged compounds have been reported, including different metal ions in various dimensionalities.[1,2] In an effort to be concise, this work is restricted to the study of azido double-bridge copper(II) dinuclear systems. In these systems, the azido groups bridge the copper(II) ions either through one terminal nitrogen atom (μ-1,1), in a so-called end-on coordination mode (abbreviated hereafter EO),[3–16] or through two terminal nitrogen atoms (μ-1,3) in an end-to-end coordination mode (EE) as shown in Scheme 1.[11,17–23]
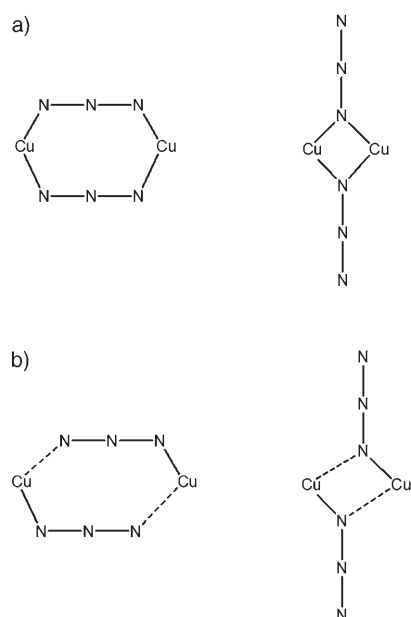
For both EO and EE systems, the bridge may be either symmetric (Scheme 1a), when the two N–Cu bonds are

a)

b)

Scheme 1. a) Symmetric and b) asymmetric end-to-end ($\mu_{1,3}$) and end-on ($\mu_{1,1}$) coordination modes.

equivalent and short (≈ 1.97–2.02 Å), or asymmetric (Scheme 1b), when the N—Cu bond is short (≈ 1.97–2.02 Å) and long (≈ 2.25 –2.66 Å). Most EO systems are symmetric,[3–5,7–10,24] whereas EE systems are generally asymmetric.[11,17,19,21–23]

From the magnetic point of view, a key distinction has long prevailed between the EO and EE coordination modes. In early studies, the EO coordination mode was systematically found to be symmetric and to exhibit ferromagnetic Cu—Cu interactions. In contrast, for the EE systems (Table 1) the interactions were found to be zero[19] or weakly antiferromagnetic[11,17,21] ($J < -100$ cm^{-1}) for the asymmetric bridge. In the few cases where the double bridge is symmetric, the copper(II) ions are so strongly antiferromagnetically coupled that the compounds appear to be diamagnetic at room temperature ($J > -300$ cm^{-1}).[20,25] In the last five years, this picture has changed somewhat be-

cause more azido-bridged copper(II) dinuclear complexes have been reported. Some asymmetric EO systems[11–13] have now been found that exhibit antiferromagnetic Cu—Cu interactions, while several cases of ferromagnetic couplings have been reported for asymmetric EE systems.[11,22,23]

In the early studies,[3–6,17–20] the symmetric EO coordination mode behavior seemed intrinsically ferromagnetic and independent of any structural parameters. This is why most previous theoretical studies focused on EO systems to explain such peculiar behavior,[24,26–30] which was initially attributed to spin polarization effects.[28,30] However, a polarized neutron diffraction study has shown that spin delocalization is indeed the main effect and that spin polarization occurs only within the azido bridge.[24] Meanwhile, the magnetostructural independence of the ferromagnetic coupling was experimentally ruled out by Thompson et al who synthesized a series of dinuclear copper(II) complexes incorporating one symmetric μ-1,1-azido bridge and one bridging diazine ligand to tune the opening of the Cu-N-Cu bridge angle. From their results, they were able to predict that the symmetric EO coordination should lead to antiferromagnetic coupling for large Cu-N-Cu bridging angles ($\theta >$ 108°).[31–33] This was further confirmed by calculations on symmetric EO models that also predicted antiferromagnetic interactions for θ angles larger than 100°.[26,27] However, no such doubly bridged symmetric EO has been obtained so far.

In comparison, the EE compounds obviously attracted very little attention[34] because they were first reported to exhibit antiferromagnetic behavior,[11,17,19–21,25] which is less relevant to magnetic materials. Moreover, at first sight, the antiferromagnetic coupling of the EE system seemed to be easy to explain if only the copper(II) coordination geometry and the bonding mode of the azido group were taken into consideration.[28] Thus, the strong antiferromagnetic interaction of symmetric EE systems was ascribed to the six-coordinate environment of the copper(II) ions with the two bridging azido groups favoring strong overlap between the $d_{x^2-y^2}$ magnetic orbitals.[20,25] In the case of asymmetric EE systems, in which the copper generally has a square-pyramidal geometry, one terminal azido nitrogen atom points to the $d_{x^2-y^2}$ magnetic orbital of one copper and the other to the d_{z^2} orbital of the second copper. This, combined with the long apical Cu—N$_{azido}$ bonds, was believed to give negligible interactions for pure square-pyramidal geometries that become sizeable antiferromagnetic interactions when the system evolves to a trigonal-bipyramidal geometry.[19,28] However, this interpretation appears no longer valid owing to the quite recent discovery of asymmetric EE systems showing ferromagnetic

Table 1. Selected magnetostructural data for asymmetric end-to-end azido double-bridged copper(II) dinuclear complexes a with square-pyramidal coordination geometry.

Compound[a]	J[b][cm^{-1}]	R[c][Å]	D[d][Å]	τ[e]	Δ[f]	Ref.
[Cu$_2$(Medpt)$_2$(μ-N$_3$)](ClO$_4$)$_2$ (**2**)	-105.2	2.093(3)–2.309(3)	5.30	0.23	11.3	[11]
[Cu$_2$(Me5dien)$_2$(μ-N$_3$)$_2$](BPh$_4$)$_2$	-13.0	1.985(4)–2.252(5)	5.23	0.29	5.15	[17]
[Cu$_2$(Me5dien)$_2$(μ-N$_3$)$_2$](ClO$_4$)$_2$	-7.5	1.996(3)–2.327(3)	5.29	0.23	30.3	[21]
[Cu$_2$(EtMe4dien)$_2$(μ-N$_3$)$_2$](ClO$_4$)$_2$	-3.6	1.996(3)–2.276(3)	5.29	0.28	31.0	[21]
[Cu$_2$(tBupy)$_2$(μ-N$_3$)$_2$](ClO$_4$)$_2$	0	1.979(5)–2.456(6)	5.00	0.21	53.1	[19]
[Cu$_2$(Et$_3$dien)$_2$(N$_3$)](ClO$_4$)$_2$	$+9.0$	2.009(5)–2.379(7)	5.41	0.20	35.8	[11]
[CuL$_2$(N$_3$)$_2$] (**1**)	$+16.0$	2.000(2)–2.356(2)	5.11	0.18	47.4	this work
[Cu$_2$(bben)$_2$(μ-N$_3$)$_2$(N3)](ClO$_4$)$_2$	$+16.8$	2.044(4)–2.373(4)	5.28	0.18	37.4	[23]

[a] Ligands: Medpt = 5-methyldipropylenetriamine; Me5dien = 1,1,4,7,7-pentamethyldiethylenetriamine; EtMe4dien = 4-ethyl-1,1,7,7-tetramethyldiethylenetriamine; tBupy = p-tert-butylpyridine ; bben = 1,2-bis(benzylamino)ethane; Et$_3$dien = 1,4,7-triethyldiethylenetriamine. [b] Magnetic coupling: $H = -JS_1S_2$. [c] R: N—Cu bond length in the azido bridge. [d] D: Cu—Cu distance. [e] τ: Addison parameter.[44] [f] Δ: torsion angle Cu-N-N-Cu.[23] All structural parameters have been calculated from the CIF files obtained from the CCDC.

behavior.[11,22,23] It now appears that magnetostructural relationships in asymmetric EE compounds are considerably more subtle. As evidenced from Table 1, several structural parameters have to be considered: not only the coordination geometry,[34] but also the Cu−N bond lengths or the Cu-N-N-Cu torsion angle, as recently pointed out.[11,23] Obviously, the azido bridge is non-innocent in the exchange process[29] Therefore, even weak ferromagnetic coupling in EE systems still deserves attention.

In the course of our work on polynuclear systems,[35–37] we synthesized an asymmetric EE azido double-bridged copper(II) dinuclear complex $[Cu_2L_2(N_3)_2]$ (**1**) with ligand (L) (Scheme 2). Interestingly, the magnetic study of this compound revealed a novel example of ferromagnetic interaction for this EE azido system. To better understand the mechanism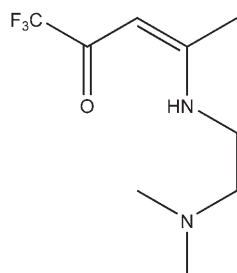 of the magnetic exchange and to clarify the role of the azido group, we studied this system by means of polarized neutron diffraction. Such a study has been previously reported for an EO[24] compound, but not for an EE system, despite the relevant information it may bring with respect to spin delocalization.[24,38–43] We also performed complementary spin-density calculations using the DFT formalism. We also carried out correlated ab initio calculations to obtain information on the electronic mechanism of the magnetic interaction.

Scheme 2. Ligand (LH).

Results and Discussion

Description of the X-ray structure at 150 K: The structure consists of discrete neutral and centrosymmetric dinuclear units (Figure 1) with a Cu−Cu distance of 5.105(1) Å. The azido groups bridge in a asymmetric EE fashion (μ-1,3) with a short and a long Cu−N bond (Cu−N5 2.000(2), Cu−N3 2.356(2) Å). As generally observed, the copper(II) ions are five-coordinate, and the coordination polyhedron is best de-

Figure 1. Molecular structure of **1**.

scribed as square pyramidal from the Addison parameter τ of 0.18.[44] The square base consists of one oxygen atom (O1), two nitrogen atoms (N2 and N1) that belong to ligand L, and one nitrogen atom (N3) from one bridging azido group. The apical position is occupied by the terminal nitrogen atom (N5) of the second azido bridge with a long Cu−N bond length (Cu−N3 2.356(2) Å). The deviation of the copper(II) ion from the mean plane of the square base (O1-N1-N2-N5) is 0.18 Å. The angle between the square base (O1-N1-N2-N5) and the (N3-Cu-N5) plane is 90.69°. The Cu-N5-N4 angle is 117.8(1)°. The azido group is almost linear (∢N3-N4-N5 177.80°). The six-membered ring formed by the two copper(II) ions and the two azido groups displays a chair-type conformation with a dihedral angle (δ) between the (N6) and (CuN2) planes[34] of 29.01 (7)° and a torsion angle Cu-N-N-Cu (Δ)[23] of 47.4 (3)°.

Description of the structure determined by elastic neutron scattering at 30 K: The cell parameters refined at 30 K (Table 2) show a contraction of the cell that occurs between

Table 2. Crystal data and structure refinement for $[Cu_2L_2(N_3)_2]$.

Crystal data		
formula	$C_{18}H_{28}Cu_2F_6N_{10}O_2$	
formula weight	657.6	
crystal system	monoclinic	
space group	$P2_1/n$ (No. 14)	
color	green	
Z	2	
Data collections and refinement details		
	X-rays	neutrons
T [K]	150	30
a [Å]	10.596(5)	10.472(1)
b [Å]	9.545(5)	9.542(1)
c [Å]	13.590(5)	13.310(1)
β [°]	107.87(5)	106.38(1)
V [Å³]	1308(1)	1276.0(2)
ρ [g cm^{-3}]	1.711	1.754
GOF on F^2	1.05	1.12
no. of reflections used	2800	2316
$R(F)$[a]	0.033 [$I > 3\sigma(I)$]	0.058 [$I > 3\sigma(I)$]
$R_w(F)$[b] all data	0.0418 [$I > 3\sigma(I)$]	0.057 [$I > 3\sigma(I)$]

[a] $R(F) = \Sigma ||F_o| - |F_c|| / \Sigma |F_o|$. [b] $Rw(F) = \Sigma [w((F_o - F_c)^2 / \Sigma w F_o^2]^{1/2}$.

150 and 30 K along the a and c crystallographic directions, whereas the b cell parameter remains constant. Nevertheless, the molecular structure is very similar to that determined by X-ray diffraction at 150 K. A comparison between selected bond lengths and angles at 150 and 30 K is summarized in Tables 3 and 4. A slight contraction (1%) of the bond lengths is observed between the copper(II) center and its first neighbors, except for the Cu−N3 bond. The N−N distances of the N_3 groups increase by 1% between 30 K and 150 K.

Magnetic behavior: At room temperature, χT (0.85 cm³ K mol^{-1}) corresponds to the expected value for two copper(II) ions (0.75 cm³ K mol^{-1}, $g = 2.13$) (Figure 2). On

Table 3. Selected interatomic distances [Å] for $[Cu_2L_2(N_3)_2]$ at 150 K (X-rays) and 30 K (neutrons).[a]

	150 K	30 K
Cu1−N1	1.961 (2)	1.9457(2)
Cu1−N2	2.035 (2)	2.0179(2)
Cu1−O1	1.927 (2)	1.9092(2)
Cu1−N3	2.356 (2)	2.3663(3)
Cu1−N5	2.000 (2)	1.9904(2)
N3−N4	1.156 (2)	1.1691(2)
N4−N5	1.188 (2)	1.2030(2)
Cu1−Cu1i	5.105(1)	5.1042(5)

[a] Symmetry transformations used to generate equivalent atoms: i) $-x,-y,-z$.

Table 4. Selected angles for $[Cu_2L_2(N_3)_2]$ at 150 K (X-rays) and 30 K (neutrons).[a]

	150 K	30 K
N1-Cu1-N2	85.25(8)	82.95(1)
N2-Cu1-N3	91.22(8)	91.28(1)
N2-Cu1-N5	90.35(7)	92.23(1)
N1-Cu1-O1	93.70(7)	96.11(1)
N3-Cu1-O1	94.13(7)	94.13(1)
Cu1-N3-N4	131.8(1)	130.69(1)
N4i-N5i-Cu1	117.8(1)	116.74(1)
N1-Cu1-N3	99.51(6)	99.49(1)
N1-Cu1-N5	163.83(7)	163.54(1)
N3-Cu1-N5	96.12(6)	96.33(1)
N2-Cu1-O1	174.65(6)	174.59(1)
N5-Cu1-O1	89.24(7)	87.21(1)
N5-N4-N3	177.7(2)	177.48(1)

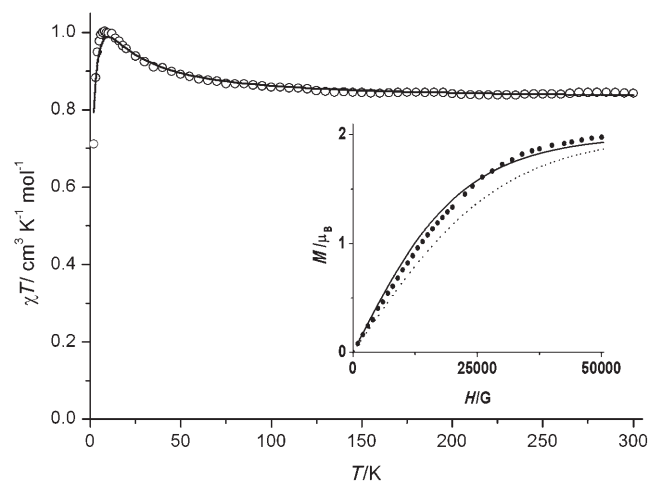[a] Symmetry transformations used to generate equivalent atoms: i) $-x,-y,-z$.

Figure 2. Temperature dependence of the χT product for **1** (○) measured in a magnetic field of 0.5 T. The solid line gives the best fit of the data with values in the text ($g=2.096(4)$, $J=+16.0(5)$ cm^{-1}, $\theta=-0.77(2)$ cm^{-1}). Inset: field dependence of the magnetization at 2 K (●) with Brillouin function for a spin $S=1$ (——) and two spins $S=0.5$ (-----).

cooling, χT increases continuously to 8 K, where it peaks (1.05 cm^{3}K mol^{-1}), which is in agreement with the maximum value expected for two copper(II) atoms that are ferromagnetically coupled ($S=1$). The decrease observed at lower

temperatures is ascribed to weak interdinuclear antiferromagnetic interactions. The magnetic susceptibility data were fitted with a simple isotropic dimer Heisenberg model ($H = -JS_1S_2$) to give a ferromagnetic interaction $J = +16.0(5)$ cm^{-1} with $g=2.096(4)$ and a small interdimer interaction $\theta=-0.77(2)$ cm^{-1}, in agreement with the long interdimer distances. The ferromagnetic coupling was confirmed by the magnetic field dependence of the magnetization at 2 K that saturates at 2 μ_B and follows the Brillouin function for a triplet ground state (Figure 2). Such a ferromagnetic interaction is difficult to predict on the basis of the coordination geometry alone.[28] Indeed, as shown in Table 1, complexes with quite close Addison parameters (0.18–0.29) may show opposite signs for the magnetic interaction. Moreover and naively, the long Cu−N bond (2.356(2) Å) in our complex would be expected to switch off any interaction; however, this is not the case. Of course, the geometry is important and may account for the relative weakness of the interaction in asymmetric EE systems. However, the sign (antiferro- or ferro-) and strength of the interaction are obviously attributable to small changes in other structural parameters. Xie et al.[23] have previously proposed that the Cu-N3-Cu torsion angle (Δ) should be taken into account. Interestingly, our ferromagnetic coupling ($J=+16$ cm^{-1}) is close to the value found by the same authors[23] for the azido complex $[Cu_2(bben)_2(\mu-N_3)_2(N_3)](ClO_4)_2$ (bben = 1,2-bis(benzylamino)ethane) for which the τ and Δ parameters are close to those we found for our compound (Table 1). The influence of the Δ parameter may be explained as it involves the azido bridge, which is obviously non-innocent in the interaction mechanism. This led us to study the spin localization in our system both experimentally, by polarized neutron diffraction, and theoretically in order to clarify the role of the azido bridge as a magnetic coupler.

Spin-density reconstruction: The spin density was reconstructed from the experimental magnetic structure factors with help of a model refinement.[45] This model describes the spin density by summing the atomic spin densities [Eq. (1)]:

$$\rho(\vec{r}) = \sum_i \rho_i(\vec{r}_i) \tag{1}$$

Each atomic density is expressed by a development on a basis of multipole functions, which was limited here to the spherical term for the N and O [Eq. (2)]:

$$\rho_i(\vec{r}) = P_{00}\mathcal{N}r^2 e^{-\zeta_i\kappa_i r} \tag{2}$$

Spherical atomic spin densities were refined on the N and O sites, with radial coefficients taken from literature $\zeta_N=3.83$ and $\zeta_O=4.45$ au^{-1}.[46] For the Cu atom, a 3d orbital model[47] was refined with local axes defined by $z \parallel$ N3Cu, $x \perp$ to (N3Cu, N2O1) and $y \perp (x, z)$ [Eq. (3)].

Table 5. Experimental (neutrons) and theoretical (DFT and DDCI-3) spin populations [μ_B] and agreement factors.

Atom	Neutrons	DFT	DDCI-3
Cu1	0.719(6)	0.571	0.806
O1	0.043(5)	0.077	0.044
N1	0.044(5)	0.100	0.028
N2	0.076(6)	0.113	0.021
N3	0.033(7)	0.113	0.040
N4	0.004(5)	−0.022	0.004
N5	0.029(6)	0.044	0.039
sum	0.95(2)	0.997	0.982
no. obs	123		
no. parameters	11		
GOF	1.6		
$R_w(F_M)$	0.079		

$$\Psi_{3d}(\vec{r}) = R_{Cu}(r)(a_1 d_{xy} + a_2 d_{xz} + a_3 d_{yz} + a_4 d_{z^2} + a_5 d_{x^2-y^2})$$

(3)

where $R_{Cu}(r)$ is a Slater-type radial function [Eq. (4)]:

$$R_{Cu}(r) = \mathcal{N} r^2 e^{-\xi_{Cu}\kappa_{Cu}r}$$

(4)

where κ_{Cu} is a contraction coefficient that can refined.

The Cu radial Slater orbital exponent ξ_{Cu} was taken equal to 4.4 au^{-1}.[46] The radial expansion coefficient κ was refined for the Cu atom. A weighted agreement factor $R_w(F) = 0.079$ and a goodness of fit GOF $= 1.6$ were obtained in the model refinement based on 123 experimental magnetic structure factors . The refined spin populations are reported in Table 5.

The sum of the populations accounts for 0.95(2) μ_B per Cu unit, a value which corresponds to an almost complete saturation, as expected from magnetic measurements. The spin delocalization onto the ligands represents 24% of the total moment on the molecule. The spin populations observed on the azido nitrogen N3 and N5 coordinated to the Cu center are slightly smaller than the populations on the nitrogen atoms N1 and N2 of the external ligands. No significant density was observed on the central nitrogen atom N4 of the azido bridges.

The refined 3d orbital coefficients of the copper ion are given in Table S1. The most important contribution is found in the $3d_{x^2-y^2}$ orbital (0.78), but small populations are also obtained in the four other 3d orbitals. The existence of spin delocalization towards the N3 atom, which lies in an axial position, is in agreement with the significant population of the d_{z^2} orbital (−0.38). The corresponding spin-density maps in the xy, yz, and xz planes relative to the local axes of one copper atom are represented in Figures S1–S3.

The spin-density map for the whole molecule is shown in Figure 3 as a projection along the crystallographic b axis. This map shows that the spin density localized on the copper centers lies essentially in the equatorial O1-Cu-N1-
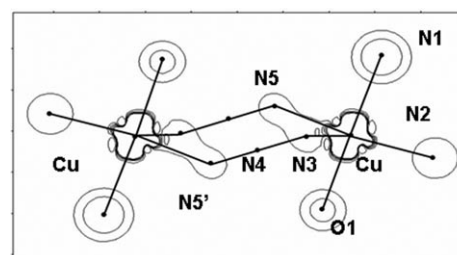

Figure 3. Experimental induced spin density in **1** at 2 K in a field of 5 Tesla projected along the b axis. Low levels only: from 0.02 μ_B Å^{-2} to 0.1 μ_B Å^{-2} in steps of 0.02 μ_B Å^{-2}.

N2-N5 plane, with an elongation along the N2−O1 bond. A stronger delocalization can be noticed on the N2 and O1 first neighbors with respect to the other neighbors. The larger population transfer from the copper to the nitrogen atoms than to the oxygen atoms is in agreement with the stronger covalent character of the Cu−N bond with respect to the Cu−O bond.[48]

Theoretical calculations: All our results, DFT and correlated ab initio, are summarized in Table 6. Whatever the basis set extension, the DFT calculations agree reasonably well with

Table 6. Coupling constants J [cm^{-1}] in complexes **1** and **2** computed using several computational methods. Spin polarization (SP) $= J_{DDCI-1} - J_{CASSCF}$, dynamical correlation (DC) $= J_{DDCI-3} - J_{CASSCF} - $ SP.

	DFT	CASSCF	DDCI-1	DDCI-2	DDCI-3	SP	DC	Exptl.
1	29.8	2.6	14.7	15.2	19.0	12.1	4.3	16.0
2	−13.0	−5.4	−9.7	−13.6	−18.3	−4.3	−8.6	−105

an energy difference of about 30 cm^{-1} between the single and triplet states, which supports the ferromagnetic nature of the interaction. Moreover, the analysis of the DFT spin density (Figure 4) shows that the main projection of the nat-
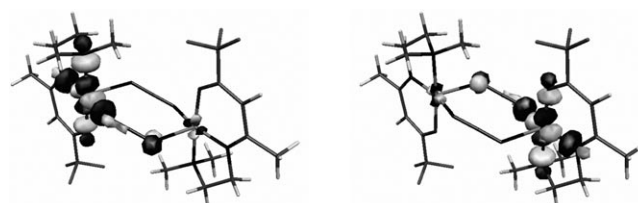

Figure 4. Natural orbital projections of the singly occupied triplet MOs (SOMOs) of dimer **1**.

ural magnetic orbitals of the triplet ground state corresponds to the $d_{x^2-y^2}$ component (≈ 0.6) which agrees well with the polarized neutron diffraction experiment (Table 5).

To obtain a better understanding of the ferromagnetic behavior in our compound [Cu$_2$L$_2$(N$_3$)$_2$] (**1**), we performed similar calculations on an analogous complex [Cu$_2$(Medpt)$_2$-(μ-N$_3$)$_2$](ClO$_4$)$_2$ (**2**; Medpt = 5-methyldipropylenetriamine), previously synthesized by Escuer et al.[11] (see Figure S4),

that exhibits antiferromagnetic behavior (Table 1). Indeed, both complexes have square-pyramidal geometries with close Addison parameters (0.18 (**1**) and 0.23 (**2**)). Thus, any analysis based on traditional concepts (i.e. two electrons in two orbitals) should lead to similar magnetic behaviors. Nevertheless, in agreement with experimental results and previous calculations,[27] our calculation for **2** gave an antiferromagnetic coupling ($J_{calcd} = -13$ cm^{-1}), despite the fact that the computed spin-density projections of **1** and **2** are very similar. Finally, the Kohn–Sham singly occupied MOs (SOMOs) provide important contributions to the azido bridge (Figure 5) in both complexes. Interestingly, the
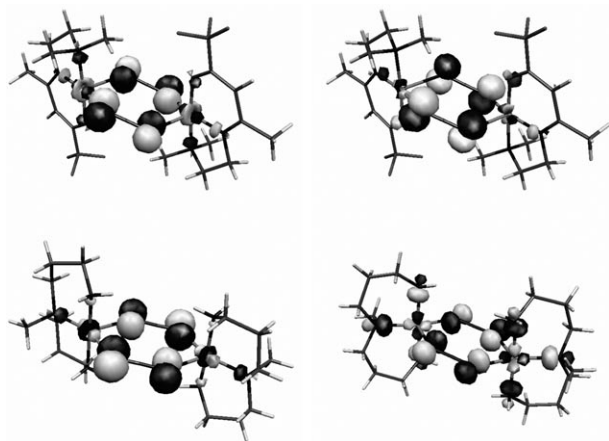

Figure 5. Kohn–Sham triplet SOMOs of the ferromagnetic and antiferromagnetic dimers **1** (top) and **2** (bottom).

energy difference between such orbitals is smaller for the antiferromagnetic complex **2** (163 meV) than for our ferromagnetic one **1** (245 meV), in contrast with the naive prediction based on a monoelectronic picture.

The sign of the magnetic interactions were confirmed by our Difference Dedicated Configuration Interaction (DDCI) calculations for both **1** and **2** (Table 6). On top of the CAS(2,2) calculations (so-called valence-only description), the iterated DDCI-1 MOs incorporate spin polarization (SP) effects (labeled as "double-spin polarization" in the original paper of de Loth et al.[49]), which clearly dominate the magnetic interaction in **1**. Such contributions account for the polarization of the inactive orbitals (i.e. doubly occupied at the CASSCF level) and particularly those of the bridging azido units involving typical π–π* excitation. We should mention that the active MOs correspond to the in-phase and out-of-phase linear combinations of the Kohn–Sham SOMOs. Our analysis is to be compared with the observation in **2** where the dynamical correlation contribution is the leading one. Even at the CASSCF level, the magnetic behavior of **2** is antiferromagnetic, while the magnetic orbitals are again very similar to those of **1**.

Analysis of the ab initio wavefunction allowed us to clarify the mechanism favoring one state over the other in complexes **1** and **2**. The highest MOs g and u are mainly the in-phase and out-of-phase combinations of the Cu $d_{x^2-y^2}$ AOs. The triplet state wavefunction T^u reads $|gu|$, whilst the lowest singlet S^g is a mixture of $|g\bar{g}|$ and $|u\bar{u}|$ determinants, $\lambda |g\bar{g}| - \mu |u\bar{u}|$. A standard MO transformation can be used to equally analyze the wavefunction in terms of the localized MOs $a = (1/2)^{1/2}(g+u)$ and $b = (1/2)^{1/2}(g-u)$. Within this valence bond picture, the coefficient of the ionic forms in S^g (i.e. $|a\bar{a}|$ and $|b\bar{b}|$) reduces to $\lambda - \mu$. From our correlated calculations, this value approaches zero $\lambda \approx \mu \approx 0.71$) in complex **1**, whereas it survives in complex **2**. Clearly, the suppression of the ionic contribution, which stabilizes the singlet over the triplet state, affects the coupling constant. The significant reduction of the torsion angle Δ in **2** (11.3°) as compared to that in **1** (47.4°) makes all contributions (CASSCF, SP and DC, see Table 1) negative in **2**. These results support the important role of the torsion angle parameter (Δ) in controlling the magnetic interaction.

Conclusion

Synthesis and characterization of a new ferromagnetic azido-bridged copper(II) complex have been reported. High-resolution polarized neutron diffraction has demonstrated the rather localized spin densities in the $d_{x^2-y^2}$ orbitals of the Cu atoms. DFT and correlated ab initio calculations have confirmed the ferromagnetic nature of the interactions and showed the highly sensitive character of the exchange coupling to the local environment by comparing results in our system **1** and the analogous **2**. The importance of spin-polarization effects along with negligible ionic contributions dominates the exchange interaction in **1**, which turns out to be ferromagnetic as observed experimentally. These results show that the nature of the magnetic interaction cannot always be predicted a priori since subtle contributions arise from mechanisms that do not stay in the valence-only space.[50,51] These results demonstrate the need for such versatile compounds to improve our understanding of magnetic systems.

Experimental Section

Synthesis: All chemicals and solvents were used as received; all preparations and manipulations were performed under aerobic conditions.

Synthesis of the ligand (LH): 1,1,1-Trifluoro-2,4-pentanedione (1 mL, 8.24 mmol) was dissolved in methanol (20 mL) and cooled on an ice bath. *N,N*-Dimethylethylendiamine (0.95 mL, 8.65 mmol) was added under agitation. The mixture was allowed to warm to room temperature, and agitation was maintained for 12 h. After removal of the solvent under vacuum, an oily yellow material was collected that was used without further purification.

*Synthesis of the complex [Cu$_2$L$_2$(N$_3$)$_2$] (**1**)*: A solution of Cu(ClO$_4$)$_2$·6H$_2$O (0.37 g, 1 mmol) in methanol (10 mL) was added to a solution of the ligand (LH; 0.224 g, 1 mmol) in methanol (10 mL) with triethylamine (0.2 mL, 1.4 mmol). To the resulting blue-green solution was added a solution of NaN$_3$ (65 mg, 1 mmol) in methanol (10 mL). The resulting deep green solution was slowly evaporated over a period of 10 days to give green plate-shaped crystals that were suitable for single-crystal X-ray dif-

fraction and which were isolated upon filtration. Yield: 52%; elemental analysis calcd (%) for $Cu_2N_{10}C_{18}O_2F_6H_{28}$ ($M = 657.6\ g\,mol^{-1}$): Cu 19.3, C 32.9, H 4.29, N 21.3; found: Cu 19.4, C 32.6, H 4.32, N 19.7. Large crystals suitable for neutron diffraction were obtained in a similar way after three weeks of slow evaporation.

Caution: Although we did not experience any problems with the compound reported in this work, perchlorate salts and sodium azide are often explosive and should be handled with great care.

Magnetic measurements: Magnetic measurements were carried out on bulk polycrystalline samples using a Teflon capped basket as sample holder with a Quantum Design MPMS SQUID magnetometer. The data were corrected for the diamagnetism of the sample holder and the diamagnetism of the constituent atoms by means of Pascal constants ($\chi_{dia} = -320 \times 10^{-6}$ cgs).

X-ray diffraction structure determination

Data collection: Diffraction data were collected at room temperature by means of the COLLECT program.[52] Lorentz-polarization correction, peak integration, and background determination were carried out with the DENZO[53] program. Frame scaling and refinement of the unit-cell parameters were performed with the SCALEPACK program.[53] The lattice constants were refined by a least-square refinement of 2800 reflections ($2.15° < \theta < 28.1°$). No absorption correction was applied to the data sets.

Structure solution and refinement: $[Cu_2L_2(N_3)_2]$ crystallizes in the monoclinic system. According to the observed systematic extinctions, the structure was solved in the $P2_1/n$ space group (no. 14) by direct methods using the SIR 97 programs[54] combined to Fourier difference synthesis and refined against F by means of reflections with $[I/\sigma(I) > 3]$ and the CRYSTALS program.[55] All thermal atomic displacements for non-hydrogen atoms have been refined anisotropically. X-ray crystallographic data and refinement details are summarized in Table 2. Selected interatomic distances and angles are listed in Table 3 and Table 4, respectively.

Neutron diffraction structure determination

Data collection: A single crystal of size ($4 \times 2 \times 1$ mm) with the long dimension along the b crystallographic axis was set on the four-circle diffractometer 5C2 of the Laboratoire Léon Brillouin (LLB) and cooled to 30 K. The data collection details are reported in Table 2. The wavelength was 0.832 Å. The cell parameters refined at 30 K were: $a = 10.472(1)$, $b = 9.542(1)$, $c = 13.310$ (1) Å, $\beta = 106.38(1)°$. The data collection was performed for θ between 2.573° and 41.52°. The integrated intensities of 6050 reflections were measured leading to 5049 unique reflections, allowing the determination of the square of the nuclear structure factors $|F_N(hkl)|^2$ after data reduction. No absorption corrections were performed because of the small value of the linear absorption coefficient, estimated to be 1.748 cm^{-1}.

Structure refinement: The atomic parameters determined from X-ray diffraction at 150 K were used as starting parameters for the neutron refinement. Atomic positions and anisotropic thermal parameters were refined against F_N with CRYSTALS[55] using 2316 reflections with $|F_N| > 3\sigma$. The extinction was refined, but was found to be negligible. The refinement statistical indices are reported in Table 2.

Polarized neutron diffraction experiment: The classical flipping ratio technique was used to determine the magnetic structure factors that are Fourier components of the magnetization density.[45] A large single crystal ($6 \times 5 \times 1$ mm) was cooled to 2 K in the cryomagnet on the 5C1 polarized neutron diffractometer at the LLB with the b direction vertical. The wavelength we used was 0.84 Å. The flipping ratios were measured at 2 K under a high magnetic field of 5 Tesla. A set of 474 flipping ratios R-(hkl) was collected with $|h_{max}| = 10$, $|k_{max}| = 3$ and $|l_{max}| = 13$ leading to 147 unique reflections. The nuclear structure factors $F_N(hkl)$ calculated from the neutron structure determined in this work at 30 K were used to derive the experimental magnetic structure factors $F_M(hkl)$ from the flipping ratios. Only the reflections with a large nuclear structure factor ($|F_N| > 5.10^{-12}$ cm) were retained for the data analysis. A correction for nuclear polarization of the hydrogen nuclei by the high external magnetic field at low temperature was applied. The Cu orbital contribution to the magnetic structure factors was subtracted from the experimental quanti-

ties to obtain the structure factors attributable to spin only. The dipolar approximation[56] was used to estimate this contribution taking a mean value 2.175 for the Landé factor g deduced from the EPR measurements. A final set of 123 magnetic structure factors was obtained.

Computational details: To gain a better understanding of the microscopic phenomenon, we performed DFT and correlated ab initio calculations. Unrestricted DFT calculations were carried out with the commonly accepted hybrid functional B3LYP[57,58] available in the Gaussian 03 suite of programs[59] with extended all-electron basis sets (triple-ζ on the metal, double-ζ on the rest of the molecule).[60,61] Broken Symmetry (BS) DFT calculations have turned out to reach agreement with experiments for dinuclear copper(II) systems as well as for several families of compounds.[13,27,34] J is directly accessible using Noodlemann's expression [Eq. (5)]:

$$J = \Delta E_{ST} = (E_{BS} - E_T)/(1 + S_{ab}^2) \tag{5}$$

where E_{BS} and E_T are the energies of the fictitious (i.e. not physical) BS and triplet states, respectively,[62] S_{ab} is the overlap between the magnetic orbitals localized on each metal center. Both energies were computed using the crystallographic structure given in the Experimental Section. The calculated spin density of the triplet state was then compared to the experimental neutron-scattering data. Even though this type of calculations allows one to clarify the nature of the magnetic interaction, it does not offer a clear picture of the underlying electronic mechanism.[46] The thus correlated ab initio multiconfigurational simulations were carried out to take advantage of the relevant information conveyed by the wavefunction. Firstly, complete active-space self-consistent field (CASSCF) calculations were performed using the Molcas 5.0 package[63] to generate a reference space (CAS) which consists in the configurations that qualitatively describe the problem. Caballol et al.[50,51] showed that a CAS including two electrons in two orbitals (2,2) is recommended for the EE azido-bridged copper(II) complexes, whilst a CAS(6,4) is required to describe ferromagnetic EO analogues.[29] In the light of these previous studies, the CAS dependence was checked and a minimal CAS(2,2) was retained. Because a negligible basis set dependence has been reported,[64] a combination of (9s6p6d)/[3s3p4d] on the Cu atoms and minimal basis sets on the rest of the complex was used in our simulations. The dynamic polarization and correlation effects were then incorporated using the difference dedicated configuration interaction (DDCI) method[65] implemented in the CASDI code.[66] In the DDCI approach, one concentrates on the differential effects rather than on evaluating the absolute energies. In particular, all the double excitations from inactive molecular orbitals (MOs) to virtual ones are not included in the CI space. This type of calculations is known to produce the most accurate evaluation of magnetic exchange coupling constants in molecular as well as in solid-state materials.[29,67] The number of degrees of freedom (i.e. holes and particles) on top of the reference CASSCF wavefunction defines the successive DDCI-1, DDCI-2 and DDCI-3 levels of calculations. The physical contributions of the corresponding determinants have been debated in the literature.[50,51] Along this procedure, a common set of MOs to describe the states of interest (i.e. singlet and triplet) has to be defined. We used the triplet CASSCF MOs, which are very similar to the singlet ones. Finally, DDCI-1, DDCI-2, and DDCI-3 simulations were performed over both states to grasp the relative importance of the different physical phenomena involved in the magnetic coupling.

CCDC-619437 contains the supplementary crystallographic data for this paper. These data can be obtained free of charge from the Cambridge Crystallographic Data Centre via www.ccdc.cam.ac.uk/data_request/cif.

Acknowledgements

[1] Y. V. Rakitin, V. T. Kalinnikov, *Russ. Chem. Bull.* **2004**, *113*, 766–774.

[2] J. Ribas, A. Escuer, M. Monfort, R. Vicente, R. Cortés, L. Lezama, T. Rojo, *Coord. Chem. Rev.* **1999**, *193–195*, 1027–1068.

[3] J. Comarmond, P. Plumere, J. M. Lehn, Y. Agnus, R. Louis, R. Weiss, O. Kahn, I. Morgenstern-Badarau, *J. Am. Chem. Soc.* **1982**, *104*, 6330–6340.

[4] S. Sikorav, I. Bkouche-Waksman, O. Kahn, *Inorg. Chem.* **1984**, *23*, 490–495.

[5] M.-L. Boilot, Y. Journaux, A. Bencini, D. Gatteschi, O. Kahn, *Inorg. Chem.* **1985**, *24*, 263–267.

[6] J.-P. Costes, F. Dahan, J. Ruiz, J.-P. Laurent, *Inorg. Chim. Acta* **1995**, *239*, 53–59.

[7] G. A. Van Albada, M. T. Lakin, N. Veldman, A. L. Spek, J. Reedijk, *Inorg. Chem.* **1995**, *34*, 4910–4917.

[8] B. Graham, M. T. W. Hearn, P. C. Junk, M. Kepert, F. E. Mabbs, B. Moubaraki, K. S. Murray, L. Spiccia, *Inorg. Chem.* **2001**, *40*, 1536–1543.

[9] L. Li, D. Liao, Z. Jiang, Y. Shiping, *Polyhedron* **2001**, *20*, 681–684.

[10] J. Carranza, C. Brennan, J. Sletten, J. M. Clemente-Juan, F. Lloret, M. Julve, *Inorg. Chem.* **2003**, *42*, 8716–8727.

[11] A. Escuer, M. Font-Bardia, S. S. Massoud, F. A. Mautner, E. Penalba, X. Solans, R. Vicente, *New J. Chem.* **2004**, *28*, 681–686.

[12] J. Luo, X.-G. Zhou, S. Gao, L.-H. Weng, Z.-H. Shao, C.-M. Zhang, Y.-R. Li, J. Zhang, R.-F. Cai, *Polyhedron* **2004**, *23*, 1243–1248.

[13] S. Triki, C. J. Gomez-Garcia, E. Ruiz, J. Sala-Pala, *Inorg. Chem.* **2005**, *44*, 5501–5508.

[14] S.-Q. Bai, E.-Q. Gao, Z. He, C.-J. Fang, C.-H. Yan, *New J. Chem.* **2005**, *29*, 935–941.

[15] S. Koner, S. Saha, T. Mallah, K.-I. Okamoto, *Inorg. Chem.* **2004**, *43*, 840–842.

[16] M. S. Ray, A. Ghosh, R. Bhattacharya, G. Mukhopadhyay, M. G. B. Drew, J. Ribas, *Dalton Trans.* **2004**, 252–259.

[17] T. R. Felthouse, D. N. Hendrickson, *Inorg. Chem.* **1978**, *17*, 444–456.

[18] Y. Agnus, R. Louis, R. Weiss, *J. Am. Chem. Soc.* **1979**, *101*, 3381–3384.

[19] I. Bkouche-Waksman, S. Sikorav, O. Kahn, *J. Crystallogr. Spectrosc. Res.* **1983**, *13*, 303–310.

[20] Y. Agnus, R. Louis, J.-P. Gisselbrecht, R. Weiss, *J. Am. Chem. Soc.* **1984**, *106*, 93–102.

[21] A. Escuer, M. Font-Bardia, E. Penalba, X. Solans, R. Vicente, *Inorg. Chim. Acta* **2000**, *298*, 195–201.

[22] P. Manikandan, R. Muthukumaran, K. R. Justin Thomas, B. Varghese, G. V. R. Chandramouli, P. T. Manoharan, *Inorg. Chem.* **2001**, *40*, 2378–2389.

[23] Y. Xie, Q. Liu, H. Jiang, C. Du, X. Xu, M. Yu, Y. Zhu, *New J. Chem.* **2002**, *26*, 176–179.

[24] M. A. Aebersold, B. Gillon, O. Plantevin, L. Pardi, O. Kahn, P. Bergerat, I. von Seggern, F. Tuczek, L. Öhrström, A. Grand, E. Lelièvre-Berna, *J. Am. Chem. Soc.* **1998**, *120*.

[25] P. Chaudhuri, K. Oder, K. Wieghardt, B. Nuber, J. Weis, *Inorg. Chem.* **1986**, *25*, 2818–2824.

[26] C. Adamo, V. Barone, A. Bencini, F. Totti, I. Ciofini, *Inorg. Chem.* **1999**, *38*, 1996–2004.

[27] E. Ruiz, J. Cano, S. Alvarez, P. Alemany, *J. Am. Chem. Soc.* **1998**, *120*, 11122–11 129.

[28] M.-F. Charlot, O. Kahn, M. Chaillet, C. Larrieu, *J. Am. Chem. Soc.* **1986**, *108*, 2574–2581.

[29] J. Cabrero, C. de Graaf, E. Bordas, R. Caballol, J.-P. Malrieu, *Chem. Eur. J.* **2003**, *9*, 2307–2315.

[30] C. Blanchet-Boiteux, J.-M. Mouesca, *J. Am. Chem. Soc.* **2000**, *122*, 861–869.

[31] S. S. Tandon, L. K. Thompson, J. N. Bridson, *J. Chem. Soc. Chem. Commun.* **1993**, 804–806.

[32] S. S. Tandon, L. K. Thompson, M. E. Manuel, J. N. Bridson, *Inorg. Chem.* **1994**, *33*, 5555–5570.

[33] L. K. Thompson, S. S. Tandon, M. E. Manuel, *Inorg. Chem.* **1995**, *34*, 2356–2366.

[34] F. Fabrizi de Biani, E. Ruiz, J. Cano, J. J. Novoa, S. Alvarez, *Inorg. Chem.* **2000**, *39*, 3221–3229.

[35] C. Aronica, G. Pilet, G. Chastanet, W. Wernsdorfer, J.-F. Jacquot, D. Luneau, *Angew. Chem.* **2006**, *118*, 4118, 4775–4778; *Angew. Chem. Int. Ed.* **2006**, *45*, 4659–4662.

[36] C. Desroches, G. Pilet, S. A. Borshch, S. Parola, D. Luneau, *Inorg. Chem.* **2005**, *44*, 9112–9120.

[37] C. Desroches, G. Pilet, P. Á. Szilágyi, G. Molnár, S. A. Borshch, A. Bousseksou, S. Parola, D. Luneau, *Eur. J. Inorg. Chem.* **2006**, 357–365.

[38] P. J. Brown, A. Capiomont, B. Gillon, J. Schweizer, *Mol. Phys.* **1983**, *48*, 753–761.

[39] R. Caciuffo, O. Francescangeli, S. Melone, B. Gillon, G. Amoretti, *Physica B + C* **1992**, *180–181*, 76–78.

[40] D. Bordeaux, J. X. Boucherle, B. Delley, B. Gillon, E. Ressouche, J. Schweizer, *Z. Naturforsch. A: Phys. Sci.* **1993**, *48*, 117–119.

[41] E. Ressouche, J. X. Boucherle, B. Gillon, P. Rey, J. Schweizer, *J. Am. Chem. Soc.* **1993**, *115*, 3610–3617.

[42] M. Bonnet, D. Luneau, E. Ressouche, P. Rey, J. Schweizer, M. Wan, H. Wang, A. Zheludev, *Mol. Cryst. Liq. Cryst.* **1995**, *271*, 35–53.

[43] A. Zheludev, M. Bonnet, D. Luneau, E. Ressouche, P. Rey, J. Schweizer, *Physica B + C* **1995**, *213&214*, 268–271.

[44] A. W. Addison, T. N. Rao, J. Reedijk, G. C. Verschoor, *J. Chem. Soc. Dalton Trans.* **1984**, 1349–1356.

[45] B. Gillon, C. Mathonière, E. Ruiz, S. Alvarez, A. Cousson, T. Rajendiran, O. Kahn, *J. Am. Chem. Soc.* **2002**, *124*, 14 433–14 441.

[46] E. Clementi, D. L. Raimondi, *J. Chem. Phys.* **1963**, *38*, 2686–2689.

[47] A. Holladay, P. Leung, P. Coppens, *Acta Crystallogr. Sect. A* **1983**, *39*, 377–387.

[48] V. Baron, B. Gillon, O. Plantevin, A. Cousson, C. Mathonière, O. Kahn, A. Grand, L. Öhrström, B. Delley, *J. Am. Chem. Soc.* **1996**, *118*, 11 822–11 830.

[49] P. de Loth, P. Cassoux, J.-P. Daudey, J.-P. Malrieu, *J. Am. Chem. Soc.* **1981**, *103*, 4007–4016.

[50] C. J. Calzado, J. Cabrero, J. P. Malrieu, R. Caballol, *J. Chem. Phys.* **2002**, *116*, 3985–4000.

[51] C. J. Calzado, J. Cabrero, J. P. Malrieu, R. Caballol, *J. Chem. Phys.* **2002**, *116*, 2728–2747.

[52] COLLECT, Nonius B. V., Delft, The Netherlands, **1997**, 307–326.

[53] Z. Otwinowski, W. Minor, *Methods in Enzymology*, Academic Press, New York, **1997**, 307–326.

[54] A. Altomare, M. C. Burla, M. Camalli, G. L. Cascarano, C. Giacovazzo, A. Guagliardi, A. G. G. Moliterni, G. Polidori, R. Spagna, *J. Appl. Crystallogr.* **1999**, *32*, 115–119.

[55] D. J. Watkin, C. K. Prout, J. R. Carruthers, P. W. Betteridge, in *CRISTAL Issue 11*, CRISTAL Issue 11, Chemical Crystallography Laboratory, Oxford, UK, **1999**.

[56] G. L. Squires in *Introduction to the Theory of Thermal Neutron Scattering*, University Press, Cambridge, **1978**, p. 139.

[57] A. D. Becke, *J. Chem. Phys.* **1993**, *98*, 5648–5652.

[58] A. D. Becke, *Phys. Rev. A* **1988**, *38*, 3098.

[59] Gaussian 03, Revision C.02, M. J. Frisch, G. W. Trucks, H. B. Schlegel, G. E. Scuseria, M. A. Robb, J. R. Cheeseman, J. A. Montgomery, Jr., T. Vreven, K. N. Kudin, J. C. Burant, J. M. Millam, S. S. Iyengar, J. Tomasi, V. Barone, B. Mennucci, M. Cossi, G. Scalmani, N. Rega, G. A. Petersson, H. Nakatsuji, M. Hada, M. Ehara, K. Toyota, R. Fukuda, J. Hasegawa, M. Ishida, T. Nakajima, Y. Honda, O. Kitao, H. Nakai, M. Klene, X. Li, J. E. Knox, H. P. Hratchian, J. B. Cross, V. Bakken, C. Adamo, J. Jaramillo, R. Gomperts, R. E. Stratmann, O. Yazyev, A. J. Austin, R. Cammi, C. Pomelli, J. W. Ochterski, P. Y. Ayala, K. Morokuma, G. A. Voth, P. Salvador, J. J. Dannenberg, V. G. Zakrzewski, S. Dapprich, A. D. Daniels, M. C. Strain, O. Farkas, D. K. Malick, A. D. Rabuck, K. Raghavachari, J. B. Foresman, J. V. Ortiz, Q. Cui, A. G. Baboul, S. Clifford, J. Cioslowski, B. B. Stefanov, G. Liu, A. Liashenko, P. Piskorz, I. Komaro-

mi, R. L. Martin, D. J. Fox, T. Keith, M. A. Al-Laham, C. Y. Peng, A. Nanayakkara, M. Challacombe, P. M. W. Gill, B. Johnson, W. Chen, M. W. Wong, C. Gonzalez, J. A. Pople, Gaussian, Inc., Wallingford CT, **2004**, p. 214.

[60] A. Schäfer, C. Huber, R. Ahlrichs, *J. Chem. Phys.* **1994**, *100*, 5829–5835.

[61] A. Schäfer, H. Horn, R. Ahlrichs, *J. Chem. Phys.* **1992**, *97*, 2571–2577.

[62] L. Noodlemann, J. G. Norman, Jr., *J. Chem. Phys.* **1979**, *70*, 4903–4906.

[63] K. Andersson, M. Barysz, A. Bernhardsson, M. R. A. Blomberg, Y. Carissan, D. L. Cooper, M. P. Fülscher, L. Gagliardi, C. d. Graaf, B. A. Hess, D. Hagberg, G. Karlström, R. Lindh, P.-Å. Malmqvist, T. Nakajima, P. Neogrády, J. Olsen, J. Raab, B. O. Roos, U. Ryde, B. Schimmelpfennig, M. Schütz, L. Seijo, L. Serrano-Andrés, P. E. M. Siegbahn, J. Stålring, T. Thorsteinsson, V. Veryazov, P.-O. Widmar in *MOLCAS Version 5.0*, Lund University (Sweden), **1998**.

[64] J. Casanovas, J. Rubio, F. Illas in *New Challenges in Computational Quantum Chemistry* (Eds.: R. Broer, P. J. C. Aerts, P. S. Bagus), University of Groningen (The Netherlands), **1993**, p. 214.

[65] J. Miralles, O. Castell, R. Caballol, J. P. Malrieu, *Chem. Phys.* **1993**, *172*, 33–43.

[66] N. B. Amor, D. Maynau, *Chem. Phys. Lett.* **1998**, *286*, 211–220.

[67] I. P. R. Moreira, F. Illas, C. Calzado, J. F. Sanz, J. P. Malrieu, N. B. Amor, D. Maynau, *Phys. Rev. B* **1999**, *59*, R6593-R6596.